Topological Redox Isomers: Surface Chemistry of Zeolite-Encapsulated Co(salen) and $[Fe(bpy)_3]^{2+}$ Complexes

Carol A. Bessel[†] **and Debra R. Rolison***

Surface Chemistry Branch (Code 6170), Naval Research Laboratory, Washington, D.C. 20375-5342

Received: June 11, 1996; In Final Form: December 5, 1996[⊗]

The electroactivity of zeolite-encapsulated redox-active transition metal complexes, {M(L)}Z, was explored for Co(salen) and $[Fe(bpy)_3]^{2+}$ formed in NaY zeolite (where salen = *N*,*N*′-bis(salicylidene)ethylenediamine and bpy = 2,2′-bipyridine). The zeolite boundary was characterized via X-ray photoelectron spectroscopy (XPS) and cyclic voltammetry in nonaqueous electrolyte at either zeolite-modified electrodes (ZMEs) or a stirred microheterogeneous dispersion of the redox-modified zeolite. Voltammetric incongruities arising for {M(L)}Z studied as a ZME rather than as a dispersion are attributed to changes imposed on the redox-modified zeolite by the mechanical force used to prepare a ZME. An increase in the time in which a mixture of {$[Fe(bpy)_3]^{2+}$}NaY and carbon are either ground or pressed produces improved peak resolution and an initial but short-lived increase in the magnitude of the voltammetric peak currents. Cyclic voltammetry of a stirred dispersion of {M(L)}Z particles at a large surface area electrode yields fewer complications attributable to the electrode binders, carbons, or mechanical handling necessary to prepare a zeolite-modified electrode. Unlike its response in a ZME, {Co(salen)}NaY gives stable voltammetry for hours when characterized in a microheterogeneous dispersion. Using terminology analogous to that established in the study of zeolite-associated photochemical probes, we reconcile the range of voltammetric responses observed for a given redox-modified zeolite, both in our results and those in the literature, as due to the type of topological redox isomer expressing the electroactivity. The voltammetry obtained with both ZMEs and heterogeneous dispersions of zeolite-encapsulated transition metal complexes provides evidence for electroactivity restricted to boundary-associated complexes.

Introduction

The first syntheses of "ship-in-a-bottle" complexes within zeolites generated much interest in the effects of site isolation and steric confinement on the physical properties and chemical reactivity of the molecules trapped within the supercages of the crystalline microporous zeolite lattice.[1−5] Figure 1 illustrates the framework structure for the synthetic faujasite zeolite type Y with its characteristic pore and supercage structure and also shows a space-filling representation of supercage-entrapped square-planar transition metal complex. Zeolite-encapsulated transition metal complexes (designated as {M(L)}Z) are commonly characterized by spectroscopic techniques and elemental analyses.[1−6]

The molecular sieving properties of a zeolite in combination with its ability for cationic mobility are anticipated to contribute to the development of sterically and ionically selective materials as catalysts and sensors. The use of {M(L)}Z for electrocatalysis and chemical sensing requires insight into the mechanism(s) by which zeolite-associated sorbates undergo redox activity at or within the zeolite lattice. Advanced applications of redox-modified zeolites would be greatly facilitated should electrode-addressable, supracommunal electronic communication be demonstrated to sorbates throughout the bulk of the zeolite crystal, *i.e.*, via intrazeolitic processes.

Two possible mechanisms for electron transfer to redox species associated with zeolites, $E^{m+}{}_{(z)}$, were first proposed by Shaw and co-workers:[7]

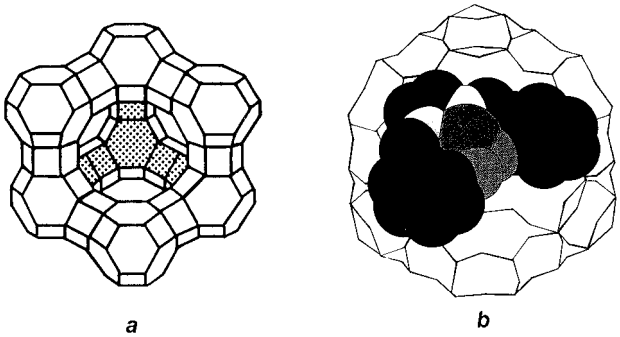

Figure 1. Framework structure of the synthetic faujasite zeolite type Y showing (a) the cage and pore architecture and (b) a supercage-entrapped transition metal complex, Co(salen), after Herron.[1]

intrazeolite mechanism:

$$E^{m+}{}_{(z)} + ne^- + nC^+{}_{(s)} \leftrightarrow E^{m-n}{}_{(z)} + nC^+{}_{(z)} \quad (1)$$

extrazeolite mechanism:

$$E^{m+}{}_{(z)} + mC^+{}_{(s)} \leftrightarrow E^{m+}{}_{(s)} + mC^+{}_{(z)} \quad (2a)$$

$$E^{m+}{}_{(s)} + ne^- \leftrightarrow E^{m-n}{}_{(s)} \quad (2b)$$

(where z = zeolite, s = solution phase, and C^+ is an electrolyte cation). The intrazeolite mechanism requires that supercage-entrapped complexes undergo electron transfer in the interior of the zeolite, but it does not specify the means whereby they do so. Since zeolites are electronic insulators and are comprised of a negatively charged lattice, the means for intrazeolite electron transfer are of considerable interest and debate. Bedioui, Balkus, and co-workers[8−17] assign the cyclic voltammetry they have observed for a range of {M(L)}Z systems to an intrazeolite

[†] National Research Council/Naval Research Laboratory Post-doctoral Associate, 1993−1995. Current address: Department of Chemistry, Villanova University, Villanova, PA 19085 (bessel@rs6chem.chem.vill.edu).

* Author to whom correspondence may be addressed (rolison@nrl.navy.mil).

[⊗] Abstract published in *Advance ACS Abstracts,* January 15, 1997.

S1089-5647(96)01716-6 CCC: $14.00

electron transfer mechanism. This mechanistic assignment remains highly controversial.[18−22]

We have recently observed electrocatalysis using {Co(salen)}-NaY species (salen = *N*,*N*′-bis(salicylidene)ethylenediammine) with benzyl chloride and CO_2 at room temperature. Compared to electrocatalysis using the same complex in homogeneous solution,[23,24] the catalyst-modified zeolites demonstrate improved selectivities, turnovers, and durability.[24] A similar improvement in catalyst durability has recently been reported for a zeolite-encapsulated Ru^{II}hexadecylfluorophthalocyanine ({Ru(F_{16}Pc)}-NaX) catalyzed oxidation of olefins using an organic peroxide as a chemical oxidant.[25] We have undertaken the present research to develop systematically optimized methods by which the variables that arise in the use of {M(L)}Z in zeolite-modified electrodes (ZMEs) or zeolite dispersions can be studied by electrochemical means.

Two transition metal complexes, Co(salen) and $[Fe(bpy)_3]^{2+}$ (bpy = 2,2′-bipyridine), were synthesized inside the supercages of NaY using the flexible-ligand methods.[1−5] These transition-metal-modified zeolites were then investigated in nonaqueous solvents, such as acetonitrile and *N*,*N*′-dimethylformamide (DMF), as monograin layers on electrodes. We have found that the mechanical work imposed (*e.g.*, by grinding or applying pressure) when preparing these materials as ZMEs affects the observed cyclic voltammetry of the monograin ZMEs.

We also investigated the cyclic voltammetry of {Co(salen)}-NaY as a stirred dispersion at a large surface area electrode (reticulated vitreous carbon, RVC). Cyclic voltammetric characterization of {M(L)}Z dispersions yields results whose interpretation is uncomplicated by the electrode binders, carbons, and handling techniques necessary to prepare a zeolite-modified electrode.[20] Both the Co^{II}-centered oxidation and reduction processes are better resolved for {Co(salen)}NaY voltammetrically characterized as a dispersion rather than as a ZME.

By considering the surface analytical and electroanalytical responses of {M(L)}Z as the above variables were explored, we have found it necessary to differentiate further the mechanisms invoked for zeolitic electron transfer in order to reconcile our results. We hope such a differentiation in mechanism, as described below, will afford a more useful language to discuss the possible sites of electron transfer for zeolite-associated redox sorbates.

Experimental Section

Chemicals and Apparatus. Solvents and chemicals were used as received unless otherwise specified: acetonitrile [Burdick and Jackson]; 2,2′-bipyridine (bpy) and $LiClO_4$ (ACS reagent grade, dried before use) [GFS]; (n-C_4H_9)$_4$NPF_6 (electrometric grade, dried before use) [Southwestern Analytical Chemicals]; *N*,*N*′-dimethylformamide (DMF), polyacrylic acid (PAA, M_w of 450 000), *N*,*N*′-bis(salicylidene)ethylenediammine (salen), dichloromethane, and anhydrous (*N*,*N*′-bis(salicylidene)-ethylenediamino)cobalt(II), Co(salen)) [Aldrich Chemical]. Ultra F Purity carbon (UPC) was obtained from Bay Carbon. $[Fe(bpy)_3](PF_6)_2$ was prepared following slight modifications of a preparation by Meyer and co-workers.[26] NaY was obtained from Strem Chemical, pre-exchanged in 0.1 M NaCl and equilibrated over NH_4Cl (aqueous saturated) before use in the synthesis of the supercage-encapsulated transition metal complexes. Reticulated vitreous carbon (RVC, 60 ppi) was obtained from Electrosynthesis, Co., cut to size, and used without pretreatment.

{M(L)}NaY materials were characterized by various spectroscopies: UV−vis (Hewlett-Packard Model 8452A diode array spectrophotometer); infrared (Mattson Research Series FTIR); X-ray photoelectron (Surface Science Instruments Model SSX-100-03, with small-spot capability, an Al anode, and at pressures of $<8 \times 10^{-9}$ Torr); inductively coupled plasma (Perkin-Elmer Plasma II emission spectrophotometer). Comparison of the UV−vis spectra for M(L) and {M(L)}Z confirmed that the expected transition metal complex formed in the zeolite, but UV−vis is an insufficiently sensitive analytical method to discern the presence or absence of low concentrations of partially formed transition metal complexes in the zeolite lattice. Furthermore, as noted previously,[22] UV−vis cannot distinguish electronic absorptions arising from complexes at the zeolite boundary from the signal dominated by intrazeolitic encapsulated complexes. FTIR confirmed the presence of uncomplexed ligand in the Soxhlet-extracted M(L)-modified zeolites. XPS and ICP were used to obtain surface and bulk elemental ratios, respectively. A {M(L)}Z sample was prepared for ICP analysis by digestion of the solid in HF, as previously described.[20] Under these acidic conditions, Co(salen) demetallates which prevents quantitative speciation of Co metal ion, uncomplexed salen, and Co(salen). Carbon and hydrogen analyses were conducted by E + R Microanalytical Laboratory, Inc. (Corona, NY).

BET surface area analyses utilized a Quantachrome Corp. Monosorb automated direct reading surface area analyzer. BET samples were prepared for analysis by heating to 250 °C for 30 h in air and storing over drierite. Immediately before analysis, samples were heated to 250 °C for 30 min under a flowing N_2 atmosphere. Samples were then sealed and transferred to an analysis station. The Quantachrome Monosorb gives a one-point determination of the amount of nitrogen adsorbed on the solid surface by sensing the change in thermal conductivity of a flowing mixture of adsorbate (N_2) and an inert carrier gas (He).

A Carver Laboratory Press Model C was used for pressure studies. Materials were either pressed in a stainless steel die or between 0.1 mm thick 316-stainless steel sheets (Goodfellow). Grinding studies used a mortar and pestle made of synthetic sapphire (with a hardness of 9+ on the moh scale) so that fewer impurities would be introduced to the sample, *i.e.*, the mortar and pestle would not itself fragment and act as an impurity in the sample.

Electrochemical measurements were conducted in a 50 mL European cell (Ace Glassware) containing a coiled Pt auxiliary, a saturated sodium chloride calomel (SSCE) or Ag/AgCl reference, and a RVC or zeolite-modified glassy carbon working electrode. The auxiliary and reference electrodes were contained in frit sticks with a D or E porosity. All solutions were purged with argon for at least 20 min before starting experiments, and a small flow of argon was present at all times. Electrochemical measurements were conducted at room temperature. Potentials were not corrected for IR drop or liquid junction potentials. Voltammetric experiments were performed with an EG&G Model 173 potentiostat/galvanostat and an EG&G Model 175 universal programmer. The output was recorded with a Yokogawa Model 3025 $x-y-t$ recorder.

Syntheses of {M(L)}Y. {Co(salen)}NaY and {$[Fe(bpy)_3]^{2+}$}-NaY were prepared as previously described.[20] The general approach to prepare {M(L)}Z is based on the "flexible-ligand" method[1] and can be summarized as follows for divalent transition metal ions such as Fe^{2+} and Co^{2+}:

$$\text{ion exchange:}\quad Na_{56}Y + xM^{2+} \underset{H_2O}{\leftrightarrow} M_xNa_{56-2x}Y + 2xNa^+$$

$$\text{chelation:}\quad M_xNa_{56-2x}Y + \text{excess L} \underset{\Delta}{\leftrightarrow} \{M(L_n)\}_xNa_{56-2x}Y$$

where x represents the atom fraction of M^{2+} ions introduced

into the zeolite and L represents the ligand coordinated to the metal center (if L = bpy, $n = 3$; if L = salen (for which $2x$ protons are generated upon chelation), $n = 1$). The ligand can sorb into the zeolite from a melt, the gas phase, or solution. {Co(salen)}NaY was prepared by two literature preparations that either do[10] or do not[1] allow exposure of the zeolite to air during the chelation step. All {M(L)}Z materials were Soxhlet extracted overnight in CH_2Cl_2 before characterization. Prior work has shown that negligible electroactivity results when air-exposed {Co(salen)}NaY is further extracted with or stirred in the polar solvent DMF.[20]

Preparation of Zeolite-Modified Electrodes. Zeolite-modified glassy carbon working electrodes were prepared by hand polishing a 3 mm diameter glassy carbon electrode (Bioanalytical Systems, Inc.) with 1.0 and 0.3 μm alumina, sonicating the electrode for 5 min each in distilled water and methanol and wiping dry with a Kimwipe. A dispersion of 10 mg of zeolite and 10 mg of carbon in 2.5 mL of methanol was sonicated for 5 min before one to two drops of this suspension was applied to the electrode surface via a disposable pipet (these layers contain 1−2 mg of zeolite and 1−2 mg of carbon). This "monograin" approach is a variation of the ZME fabrication method devised by Li and Calzaferri.[27] Carbon is used to increase the area of electrical conductor in direct contact with the zeolite. After the surface was air dried, one drop of a polyacrylic acid solution (120 mg in 15 mL of methanol) was added via a disposable pipet to overcoat the "monograin" layer on the electrode surface. The modified electrode was air dried. We attempted to use several other polymer binders such as polystyrene, polyethylene, and polyisoprene. However, we found that these polymers were neither sufficiently stable in DMF nor redox inactive to be used as a binder for our studies with these ZMEs. ZMEs of this form—PAA-overcoated {M(L)}Z/C layer—are physically durable for several hours with potential cycling in DMF and CH_3CN electrolytes.[20]

Dispersion Electrochemistry. The working electrode for our dispersion studies consisted of a piece (1 cm × 1 cm × 2.5 cm) of reticulated vitreous carbon. We found that our approaches to chemical or electrochemical treatment of used RVC electrodes did not revive the RVC sufficiently to produce clean voltammetric backgrounds, so a freshly cut piece was used for each dispersion experiment. The M(L)-modified zeolite was suspended in solution by continuous bubbling of argon through a coarse frit and concomitant mechanical stirring with a Teflon-coated stir-bar. The suspension density was 1 mg/mL.

Results and Discussion

Analyses of {Co(salen)}NaY and {Co(salen)}NaY-Modified Electrodes. CH_2Cl_2-extracted, air-exposed {Co(salen)}-NaY (as previously reported[20]) is surface-enriched in Co (Co/Al = 0.39) relative to the bulk (Co/Al ratio = 0.28 for a loading of 1.75 Co for every supercage). C/H analysis of this sample yielded 2.63% H and 11.52% C. The measured surface areas for the zeolite in various stages of modification gave the following: NaY, 624 ± 97, CoNaY, 659 ± 90, {Co(salen)}-NaY, 360 ± 85 m^2/g of zeolite.

The initial Co^{2+} ion-exchange reaction yields an equilibrium distribution of Co^{2+} throughout the zeolite lattice, but an equilibrium distribution of supercage-encapsulated complexes is unlikely, since complex formation creates diffusional roadblocks within the zeolite. This general process is depicted schematically in Figure 2. Excess ligand is also trapped within the zeolite, as confirmed by FTIR analysis of {Co(salen)}NaY, owing to diffusion hindered by M(L)-filled or ligand-filled supercages. Available pore volume in the zeolite crystal is

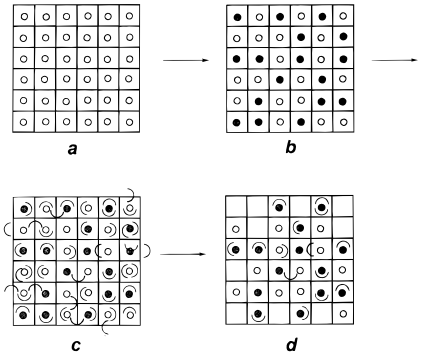

Figure 2. Schematic of the "flexible-ligand" synthesis of {M(L)}Z: (a) NaY (○ = Na^+); (b) $M_xNa_{56-2x}Y$ (● = M^{2+}); (c) intrazeolite congestion and blockage arising as the flexible ligand (∩ = L) diffuses and reacts into the zeolite interior from the zeolite boundary; (d) $\{M_x(L_n)\}Na_{56-2x}Y$ after Soxhlet extraction indicating retention of uncomplexed ligand and M^{2+}.

indeed blocked, even after a Soxhlet extraction, as evidenced by the >40% loss of surface area for CH_2Cl_2-extracted {Co(salen)}NaY over that of the ion-exchanged material, CoNaY.

The cyclic voltammetry of {Co(salen)}NaY prepared as a monograin ZME has been previously discussed.[20] Briefly, the response of a {Co(salen)}NaY-modified electrode is sensitive to the type of carbon present in the overlayer, the presence of air and moisture during chelation by the flexible ligand, and the extent and manner of postsynthetic purification of Co(salen)-modified NaY.[20] Furthermore, only *ca*. 1% of the Co(salen) complexes calculated to be formed within the zeolite exhibit electroactivity,[20,28] and the magnitude of this minimal electroactivity decays with cycling. A fractional electroactivity of 1% is not atypical for zeolite-encapsulated transition metal complexes. Although Bedioui *et al*. did not report the electroactive fraction they observed for their various {M(L)}Z studies (including {Co(salen)}NaY[10]) in their early papers,[8,10−12] in their most recent papers, they report the voltammetrically accessible fraction is maximally 5%.[13−15] Such minimal electroactivity implies that only a small amount of the encapsulated complex is available for electron transfer on the time scale of the voltammetric experiment (*ca*. 10^2 s).

Dispersion Techniques. Relying on ZMEs to obtain redox information from zeolite-encapsulated transition metal complexes is complicated by some or all of the following factors: (1) the addition of electrode binders—which may occlude the exterior pore of the zeolite, may have instability in the solvent, or may contribute potential redox signal; (2) the presence of carbon[20]—which has built-in electron transfer mediators arising from the oxygen functionalities inherent to graphitic carbons;[29] (3) the formulation or handling techniques—which usually impart mechanical work to the zeolite lattice. We now report our investigation of dispersion techniques as an alternative means to characterize {M(L)}Z.

Figure 3 demonstrates our results with CH_2Cl_2-extracted, air-exposed {Co(salen)}NaY mechanically dispersed in DMF electrolyte at a large surface area RVC electrode. Included for comparison are the background response of RVC and the homogeneous electrochemistry of Co(salen) at RVC. Several interesting differences are apparent on comparing the cyclic voltammetry of {Co(salen)}NaY as a component of a ZME[20] to that as a suspension in electrolyte. Notably, the peak currents for both the Co^{II}-centered reduction and oxidation are approximately equal when measured via dispersion electrochemistry, as are the cathodic and anodic branches for the Co^{II}-centered reduction. When {Co(salen)}NaY is studied as a ZME,

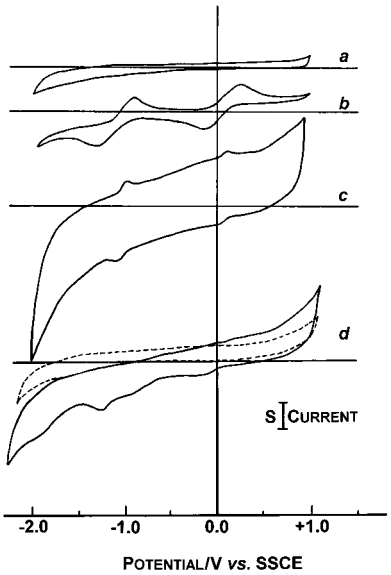

Figure 3. Dispersion cyclic voltammetry. Cyclic voltammetry in $LiClO_4$/DMF at large area RVC electrodes; scan rate = 50 mV/s. (a) blank electrolyte, $S = 1$ mA; (b) 1 mM Co(salen) in homogeneous solution, $S = 1$ mA; (c) dispersion of CH_2Cl_2-extracted, air-exposed {Co(salen)}NaY, $S = 0.25$ mA; (a−c) 0.2 M $LiClO_4$; (d) dispersion of CH_2Cl_2-extracted, air-exposed {Co(salen)}NaY after pressing for 30 min at 14 000 lb/in.^{2} (gauge), $S = 0.5$ mA, 0.1 M $LiClO_4$; - - - indicates the blank electrolyte background for the RVC used as the dispersion feeder electrode; (c, d) suspension density = 1 mg of zeolite/1 mL of solution.

an imbalance exists between both the peak current obtained for the Co^{II}-centered reduction and oxidation and the cathodic/anodic branches of the $Co^{II/I}$ couple for {Co(salen)}NaY.[20]

The peak currents for both the $Co^{II/I}$(salen) and $Co^{III/II}$(salen) couples remain stable over hours of cycling when {Co(salen)}-NaY is studied as a heterogeneous dispersion. The same redox-modified zeolite when studied as part of a ZME yielded peak currents that decreased drastically over minutes.[20] Several other groups have observed similar decreases in peak currents with voltammetric cycling at redox-modified ZMEs.[12,13,18] These decreases in peak current with time at the ZME are consistent with an extrazeolite redox mechanism in which ion exchange with electrolyte cations (or desorption by solvent) frees the redox-active species to diffuse away from the working electrode and into solution. This loss of near-surface redox solute does not readily occur when {Co(salen)}NaY is characterized by dispersion electrochemistry. Our results, as detailed below, indicate this is so because the redox-modified zeolite can be studied without any of the grinding or pressing commonly needed to form a ZME.

The formal potentials observed for {Co(salen)}NaY via dispersion cyclic voltammetry are generally not shifted from those observed in homogeneous solution nor are the ΔE_p values changed from their solution-state values. These results—plus the consistency of the dispersion peak currents with cycling and exposure to electrolyte—might indicate that a significant amount of the Co(salen) species leaches into solution from the zeolite surface or near-surface sites to provide a constant homogeneous faradaic response at the large surface area electrode. To test this, the Co(salen)-modified zeolite powder was allowed to settle out of solution and then the roughly zeolite-free electrolyte was voltammetrically tested: no faradaic response was obtained. Upon redispersing the redox-modified zeolite powder into the electrolyte, the voltammetric peaks were again visible. This simple test shows that the faradaic response, although solution-like, is zeolite-associated, providing evidence that the actual electroactive species must be related to a boundary-associated species on the zeolite.

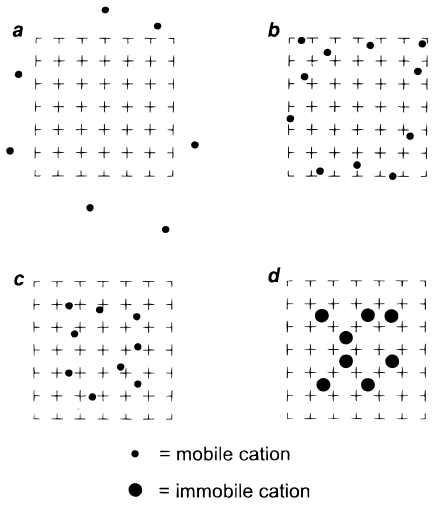

Figure 4. Schematic of the four topological isomers of zeolite + a redox probe, after the terminology assigned by Turro and Garcia-Garibay:[33] (a) outer isomer, $(R-Z)_o$; (b) boundary isomer, $(R-Z)_B$; (c) inner, global isomer, $(R-Z)_{i,G}$; (d) inner, localized isomer, $(R-Z)_{i,L}$.

A zeolite particle kept suspended by stirring in the electrolyte only has incidental contact with the surface of the RVC electrode, so sampling beyond the zeolite boundary would seem unlikely. It can be expected, though, that multiple "hits" occur on different portions of the exterior of a zeolite particle before the particle moves back into solution. Integrating the charge in the $Co^{II/III}$-centered wave of Figure 3b yields 1.9×10^{-9} mol of electroreactant for an estimated fractional electroactivity of 0.07%; integration of charge in the $Co^{II/I}$-centered wave yields 1.6×10^{-9} mol of electroreactant. This is a stable electroreactant population for 2−3 h in this electrolyte.

Topological Redox Isomers in Redox-Modified Zeolites. Based on the predominant electro*inactivity* of {Co(salen)}NaY when studied either as a ZME or dispersed solid, we must conclude that the interior molecules are voltammetrically inaccessible. The term intrazeolite has been used by zeolite scientists to describe processes occurring within the bulk or interior of the zeolite crystal;[30−32] intrazeolite thus represents >90% of the active area of the zeolite. That so few Co(salen) molecules are voltammetrically accessible, by either ZME or dispersion electrolysis, disallows the possibility that an *intra*zeolite mechanism is operative. We now need to distinguish between an extrazeolite electron transfer mechanism where the redox species physically moves beyond the zeolite crystal and one which invokes communication with redox species sited at the external ends of the zeolite crystal (*e.g.*, to complexes in defect sites or truncated or damaged cage structures).

To delineate further the mechanisms for electrochemical processes observed with redox-modified zeolites, we have adopted the terminology specified by Turro and Garcia-Garibay[33] in which they defined the topological regions of a zeolite as experienced by a photochemical probe molecule. The four possible types of topological isomers, as designated for a redox molecular probe, are illustrated in Figure 4.

Figure 4a shows $(R-Z)_o$, where the redox solute, R, is outside, o, the zeolite. Such a species is dissolved in the electrolyte solution and has no association (either bonding or sorptive) with the zeolite, although R may have originated in the zeolite. This is the isomer most closely representative of the way extrazeolite electron transfer has been heretofore defined.

Figure 4b shows $(R-Z)_B$, where R is bound to the external surface topology (or boundary B) of the zeolite. This type of isomer would include (i) size-excluded R, which is adsorbed or ion exchanged to the outer surface of the zeolite, (ii) R at the zeolite exterior, which is insufficiently desorbed or displaced during purification of a redox-modified zeolite, (iii) R adsorbed at or occluded in defect sites at the boundary, which could include truncated or partially broken zeolite supercages, and possibly (iv) R encapsulated in the first layer of complete supercages at the zeolite's outermost boundary.

Figure 4c shows $(R-Z)_{i,G}$, where R has adsorbed into the inside (i) of the zeolite crystal (*i.e.*, truly intrazeolite) but is not confined and is free to sample the global (G) pore lattice topology over the time scale of the experiment.

Figure 4d shows $(R-Z)_{i,L}$, where R is adsorption-restricted or size-included in the interior of the zeolite within a supercage, channel intersection, or cubo-octahedral (sodalite) cage (locally, L, closed).

The last two topological isomers, $(R-Z)_{i,G}$ and $(R-Z)_{i,L}$, are *intra*zeolitic in nature in that they reside within the bulk of the zeolite crystal and do not sample the exterior of the zeolite. The two inside topologies offer extreme mass transport differences, however, and should be experimentally distinguishable. This difference was discerned and demonstrated by Baker and co-workers who synthesized low loadings of Ag^I-exchanged zeolite Y ($Ag_xNa_{56-x}Y$, $x < 5.9$), where it is known that the silver ions occupy only the small channel system of the zeolite topology (*i.e.*, the hexagonal prism—sodalite cage) rather than the large channel system dominated by the supercages.[18] Chronoamperometric characterization of low-loaded Ag^INaY ZME—with its hindered Ag^+ mobility through the small channel system—yielded non-Cottrellian behavior, indicating that the process leading to the faradaic step was not diffusion-controlled in nature. The limiting step was interpreted as the hindered exchange of Ag^+ into the large channel system through the restrictive six-oxygen ring opening of the small channel system with an activation energy of 35 ± 1 kJ/mol.[18] The rapid mobility of Ag^+ in the large channel system, as seen for $Ag_xNa_{56-x}Y$ with $x > 6$, was expressed in chronoamperometry as Cotrellian diffusion-controlled electron transfer and interpreted, in conjunction with other tests, as extrazeolitic electron transfer.[18]

The first two topological isomers, $(R-Z)_o$ and $(R-Z)_B$, are *extra*zeolitic in nature, in that they do not sample the bulk of the zeolite crystal, but R present in these environments and undergoing electron transfer will clearly be subject to different mass transport and site-dependent physicochemical conditions (compare parts a and b of Figure 4). Since zeolite-encapsulated transition metal complexes do not undergo intrazeolite electron transfer in the absence of mobile intrazeolitic electron transfer mediators, such as demonstrated in the vectorial electron transfer designs of Mallouk and co-workers,[34−37] the question now becomes: is the extrazeolite electron transfer observed for {M(L)}Z due to that for a true outside isomer or a boundary isomer?

Effect of Mechanical Working of the Zeolite on Electroactivity. As discussed above, using two approaches to characterize the electrochemical response of {Co(salen)}NaY (in its near-surface Co-rich form) has yielded very different behavior: stable, long-lived voltammetric waves when {Co(salen)}NaY is characterized as a solid dispersed in electrolyte at a large area feeder electrode versus rapid loss of the initial minimal electroactivity when the same solid is studied as a ZME.[20] The electroactivity appears to be due to a durable $(\{Co(salen)\}NaY)_B$ species when the material is studied via dispersion electrolysis. Yet when studied as a ZME, $(\{Co(salen)\}NaY)_o$ would be the electroactive isomer assigned. To explain both sets of results mechanistically, a boundary isomer, which could be quite stable if strongly adsorbed or encapsulated, would have to convert to an outer isomer during the formulation necessary to prepare a modified electrode.

In order to produce effective ZMEs, a means is required by which the interphase of contact between the working electrode and the electronically insulating zeolite can be maximized. In the literature, this requirement is often addressed by grinding redox-modified zeolite with carbon to facilitate electrical contact from the electrode surface via the carbon powder to the exterior surface of the zeolite and to any near-surface (R_B) redox probe.[19,38,39] Grinding imparts mechanical work and is a plausible energetic reason for explaining the conversion of electrochemically well-defined $(\{Co(salen)\}NaY)_B$ isomers to the fleeting $(\{Co(salen)\}NaY)_o$ isomer. Gilman has recently discussed mechanochemistry (chemical reactions driven in solids by shear strain generated by mechanical force) as a means to initiate chemical reactions in solids. In addition to the thermal energy accompanying shear strain in solids, changes in orbital and structural symmetry occur and can trigger athermal reactivity.[40]

Images obtained with scanning electron microscopy (SEM) (Figure 5) show that grinding NaY zeolite for extended periods of time (>10 min) causes a noticeable reduction in the size of the average zeolite crystals from 1−10 μm to <1 μm. Furthermore, once hand ground for 60 min, the zeolite crystals exhibit obviously rounded edges. This abrasion may both break the zeolite aggregates into smaller particles and fracture bonds within the zeolite unit cell. The bond energies for the Si−O[41] and Al−O[42,43] bonds are quite large (at 298 K): 810 ± 11 and 508 ± 10 kJ/mol, respectively. However, recent work on the ball milling of zeolites (ZSM-5, A, and X;[44] and HNaY[45]) support our conclusions. Ball milling of these materials produced both the loss of zeolite crystallinity and breakage of external T−O−T bonds (T = Si or Al) of the zeolite framework.[44,45] Auroux *et al.* report that their data suggest that the supercage structure is destroyed first during the mechanically induced decrystallization.[45] In addition, Schulz-Ekloff and co-workers in an XPS study of monodispersed metal-loaded zeolites used grinding and crushing of the metal-modified zeolites to break the zeolite lattice and expose intrazeolitic metal to XPS analysis.[46]

A ZME formulation that imparts mechanical work, even under less extreme cases than above, risks creating new surface and fractured segments of the zeolite lattice and, as a consequence, should affect the status of the transition metal complexes, especially at the boundaries of the affected surfaces. If an extracrystalline mechanism is operative, the faradaic signal should be initially enhanced, since species in work-damaged environments are likely to be more mobile. The eventual loss of faradaic signal with an otherwise electrochemically stable and reversible species would also be predicted as the species diffuse away from the damaged zeolite boundary during the electrochemical experiment.

We have previously reported the effects of hand-grinding $\{[Fe(bpy)_3]^{2+}\}$NaY with UPC carbon for specified periods of time before application of the {M(L)}Z/C mixture to the electrode surface.[47] Increases in the faradaic signal for both the metal-centered oxidation and ligand-centered reduction and an improvement in the resolution of the voltammetric waves with increased grinding time were obtained, but the faradaic response for the ZME prepared from ground $\{[Fe(bpy)_3]^{2+}\}$-NaY rapidly diminished with cycling. These results are

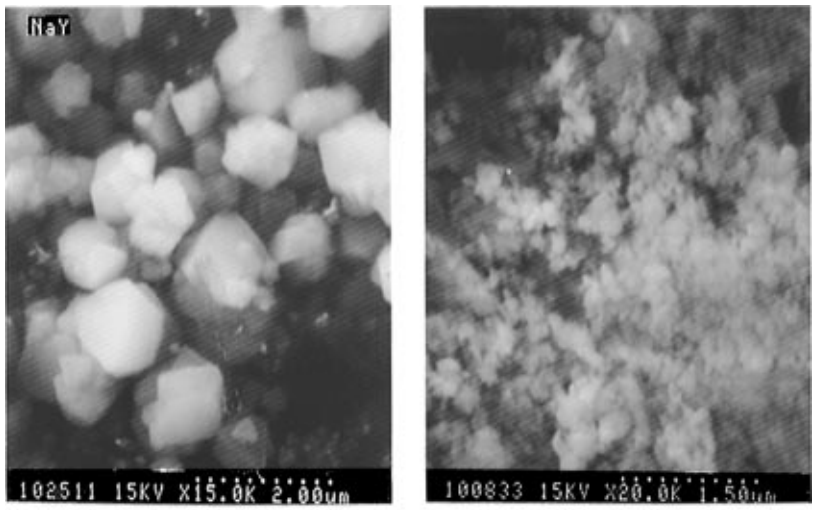

Figure 5. SEM of NaY crystals: (a) prior to grinding or pressing; (b) after grinding in a sapphire mortar and pestle for 60 min.

consistent with the electron transfer isomer being ({[Fe(bpy)$_3$]$^{2+}$}NaY)$_o$, fully in accord with the extrazeolite redox mechanism, [2], proposed by Shaw and co-workers,[7] where the zeolite-unassociated complex undergoes direct electron transfer with the electrode surface.

The method chosen by Bedioui *et al.* in their studies of zeolite-encapsulated transition metal complexes involves pressing an equal weight mixture of carbon and redox-modified zeolite into a metal grid at an unspecified pressure for an unspecified time.[8,10−17] This formulation imparts pressure work to the zeolite. It is not clear from their work if the carbon and {M(L)}Z mixture is ground together before pressing. Flanigen reports that extended hand grinding in a mortar and pestle causes damage to the crystallinity of the zeolite as does pressing dehydrated aluminosilicate zeolites at pressures greater than 20 000 psi.[48] The community studying zeolites in electrochemical interphases typically does not work with dehydrated zeolites, so the more relevant information concerns the effect of pressure on partially or fully hydrated zeolites. Freeman and Stamires have discussed that zeolites are more susceptible to crystal damage in the presence of adsorbed water.[47]

Figure 6 illustrates the changes observed in the cyclic voltammetry of ZMEs prepared by pressing a mixture of lightly ground {[Fe(bpy)$_3$]$^{2+}$}NaY (hydrated) and UPC at 14 000 lb/in.^{2} for a specified period of time before applying the mixture of {M(L)}Z and carbon to the electrode surface. As the time that the {M(L)}Z + carbon components are pressed together increases, an increase in the faradaic current and an improvement in the resolution of the peak shape again results. As was the case for grinding, the mechanical energy imparted to the zeolite lattice by pressing the carbon and zeolite mixtures should fracture portions of the zeolite lattice to expose a greater surface area to the electrolyte.

We note that the bipyridyl-centered reductions produce a larger faradaic current than does the Fe-centered oxidation. This was also seen for the prior grinding study of {[Fe(bpy)$_3$]$^{2+}$}-NaY.[47] This disparity in faradaic charge makes it appear as though more molecules undergo electron transfer for the ligand-centered processes than for the metal-centered process. This might arise if the excess bipyridyine trapped in the zeolite crystal acts as a mobile electron transfer mediator,[50] but we also note that this increase still represents a minor fraction of the intracrystalline complexes.

The effect of mechanical work on the electrochemical response of CH_2Cl_2-extracted {Co(salen)}NaY—without the ancillary issues involved in formulating a ZME—was tested by pressing the solid (unmixed with carbon) at 14 000 lb/in.^{2} for 30 min. As previously discussed, unworked {Co(salen)}NaY exhibits small, but well-defined voltammetric peaks (see Figure 3c)—characteristic of Co(salen)—that are durable for hours. The dispersion electrolysis of pressed {Co(salen)}NaY is shown in Figure 3d. The zeolite does not cohere as a self-sustaining pellet when pressed at 14 000 lb/in.^{2}, so it is readily dispersed in the electrolyte. The faradaic response is no longer characteristic of Co(salen) as a homogeneous species or as a boundary topological redox isomer. Neither the Co^{II}-centered oxidation or reduction exhibits equivalent anodic and cathodic branches; the Co$^{III/II}$(salen) couple is barely visible and a new reduction wave at −0.82 V/SSCE appears. Mechanical working of {M(L)}Z-modified electrodes produces artifactual electrochemical results uncharacteristic of the redox-modified zeolite as designed and synthesized.

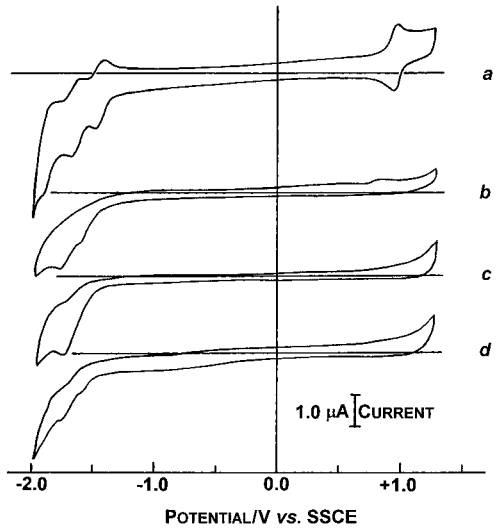

Figure 6. Pressure study. Cyclic voltammetry of homogeneous and zeolite-encapsulated [Fe(bpy)$_3$]$^{2+}$ in 0.1 M *n*-Bu$_4$NPF$_6$/CH$_3$CN at 10 mV/s: (a) [Fe(bpy)$_3$]$^{2+}$ at an unmodified GCE showing the Fe(II)-centered oxidation at +0.9 V and the three ligand-centered reductions negative of −1.3 V; (b−d) ZMEs prepared from lightly ground powders of ultrapure carbon and {[Fe(bpy)$_3$]$^{2+}$}NaY which were pressed together at 14 000 lb/in.^{2} (gauge) for the specified period of time; (b) 10 min; (c) 30 min; (d) 60 min. The first cycle was recorded.

Zeolite-Imposed Steric Confinement Effects. An often debated point in the synthesis of {M(L)}Z species involves the

TABLE 1: Formal Potentials ($E^{\circ\prime}$) and Peak Separations (ΔE_p) for Co(salen) and {Co(salen)}NaY

	$Co^{III/II}$(salen) $E^{\circ\prime}$/V (ΔE_p/mV)	new species $E^{\circ\prime}$/V (ΔE_p/mV)	$Co^{II/I}$(salen) $E^{\circ\prime}$/V (ΔE_p/mV)
Homogeneous Solution			
DMF[a]	+0.07		−1.08
CH_3CN[b]	+0.08		−1.30
Encapsulated into Zeolite			
pressed powder, CH_3CN[c]	+0.215 (71)	−0.740 (92)[d]	−1.252 (75)
ZME, DMF[e]	+0.54		−1.52
dispersion at RVC, DMF[f]	+0.08 (70)		−1.01 (65)

[a] 0.1 M $LiClO_4$ electrolyte; V *versus* SSCE. [b] 0.1 M $NaClO_4$ electrolyte; V *versus* Ag/AgCl. [c] Prepared as a pressed-powder composite in 0.1 M $TBABF_4$ electrolyte; V *versus* SCE.[10] [d] Assigned to $[Co^{III}(salen)]^+$. [e] 0.1 M $LiClO_4$ electrolyte, V *versus* SSCE.[20] [f] 0.1 M $LiClO_4$ electrolyte, V *versus* SSCE.

possibility of partially chelated moieties within the zeolite supercages. Cyclic voltammetry can be a powerful tool for determining the identity of new coordination complexes formed by ligand substitution reactions.[51] Studies by Eichhorn and Speiser[52] and by Kapturkiewicz and Behr[53] indicate that the solvation environment influences the formal potential of Co(salen) complexes by as much as 0.26−0.41 V. Changes in the potentials of zeolite-encapsulated species could give valuable information about possible binding between the encapsulated transition metal species and the zeolite as well as possible changes in ligand coordination.

Spectroscopic studies of {M(L)}Z provide data for and against supercage influence on the complex geometry and coordination. For example, DeWilde, Peeters, and Lunsford[5] reported that the absorption and emission bands (and lifetime) of $\{[Ru(bpy)_3]^{2+}\}$NaY were similar to those found in dilute, O_2-free aqueous homogeneous solutions, which implies essentially complete, unstrained $[Ru(bpy)_3]^{2+}$ complexes formed within zeolite Y. Any remaining incongruities were blamed on the formation of impurities such as $\{[Fe(bpy)_3]^{2+}\}$NaY.[5,54−56] Calzaferri and co-workers report spectroscopic evidence for partial complexation of $[Ru(bpy)_3]^{2+}$ at high loadings in NaY, finding almost pure $[Ru(bpy)_3]^{2+}$ only when the loading was less than one complex for every two supercages.[57]

Herron concluded that {Co(salen)}NaY had an oxygen affinity similar to that of the homogeneous solution state Co(salen) complex once the 1:1 pyridine adduct was formed, although O_2 binding was determined to be less favorable within the zeolite and to exhibit negative cooperativity.[1,58] On an opposite note, Schoonheydt, Jacobs, and co-workers reported the EPR and vis−near-IR spectroscopies of several zeolite-encapsulated transition metal complexes, including {Co(salen)}NaY, suggesting that partial chelation of the metal to the zeolite and to the ligand occurs.[6] {Co(salen)}NaY exhibited reflectance vis−near-IR spectroscopy consistent with complex formation. However, the EPR spectra of {Co(salen)}NaY was not temperature-dependent and exhibited two Co^{II}-dependent signals. The majority of the signal was attributed to an unidentified Co^{II} low-spin complex, since it was O_2-insensitive and unaffected by the presence of pyridine. The second signal (<1%) was O_2-sensitive and became more intense with pyridine treatment, indicating possible formation of the superoxo complex, $[Co^{III}(salen)(py)(O_2^-)]^-$. Jacobs and co-workers suggested that the formation of planar {Co(salen)}NaY species occurred only in low yield due to the steric constraints of the NaY zeolite.[6] That only *ca*. 1% of the available complexes exhibited the expected oxygen-binding behavior while the majority of the intrazeolite species did not may offer ancillary evidence that, just as in electroactivity, boundary complexes are the more reactive (because more accessible) electron transfer reactants.

In homogeneous solution the Co(salen) complex has two one-electron couples corresponding to metal-centered oxidation and reduction processes (see Figure 3b). Bedioui, Balkus, and co-workers observed several additional couples in the cyclic voltammetry of their pressed-powder {Co(salen)}NaY ZME in DMSO or CH_3CN when compared with the homogeneous Co(salen) species. They attributed these extra couples to isomers of the Co(salen) complex and proposed complexes containing partially associated salen, ligand-bridged complexes, or complexes that interact with the zeolite.[10] Their results are compared with our own in Table 1. The proposed new Co^{III}(salen) species was not observed to react with free pyridine in the electrolyte solution. The authors argued that this was indicative of a strong interaction between a $[Co^{III}(salen)]^+$ form and the zeolite, possibly caused by the partial chelation of the salen ligand or by a nonplanar ligand configuration.

Our observations using {Co(salen)}NaY as a monograin ZME or as heterogeneous dispersion contradict several of Bedioui and Balkus' conclusions. First, our cyclic voltammetric studies of {Co(salen)}NaY—either at ZMEs or with dispersion methods—do not indicate the presence of any redox couples that are not attributable to Co(salen) as it is observed in homogeneous solution. Although we do observe a shift in the $E^{\circ\prime}$ values at the ZME from those for the $Co^{III/II}$(salen) and $Co^{II/I}$(salen) redox couples in homogeneous solution (see Table 1), we see no reason to assign these shifts to new or unusual coordination modes. The shifts in potential at the ZME are similar in magnitude to those observed by Bedioui *et al*.[10] and may be due to an environmental difference once the Co(salen) species is released to the interphase of zeolite/carbon/electrolyte. It should be noted, as previously discussed by Shaw *et al*., that this interphase has a very high activity for the solute once it is displaced from the zeolite.[7]

We find far less of a deviation from the homogeneous formal potentials when {Co(salen)}NaY is characterized as a micro-heterogeneous dispersion, evidence again that the high activity of $(R-Z)_o$ in the composite environment of a ZME may affect the redox response. The observed peak separations (ΔE_p) are solution-like for {Co(salen)}NaY studied either as a ZME or as a dispersion, which again supports an extracrystalline redox mechanism. Further study and simulation of the faradaic response for the dispersed redox-modified zeolites is necessary. This form of electroanalysis offers an obverse arrangement to that customary for chemically modified electrodes in that the immobilized solute is not tethered to the electrode but rather to a micrometer-sized solid particle that must transverse the diffuse layer at the stationary, but unmodified, feeder electrode.

Finally, unlike Bedioui *et al*.,[8,10,16] we do not observe any additional redox couples indicating partially synthesized, ligand-bridging, or zeolite-bonded isomers for the boundary-sited Co(salen) or $[Fe(bpy)_3]^{2+}$ complexes. Our results are consistent with those of Herron[1] and Lunsford,[5] but since the electron transfer process is extrazeolitic in nature and does not probe the bulk of the zeolite-encapsulated complexes in the zeolite interior, it is not surprising that the voltammetry does not discern structural isomers. Should true intrazeolite electron transfer to

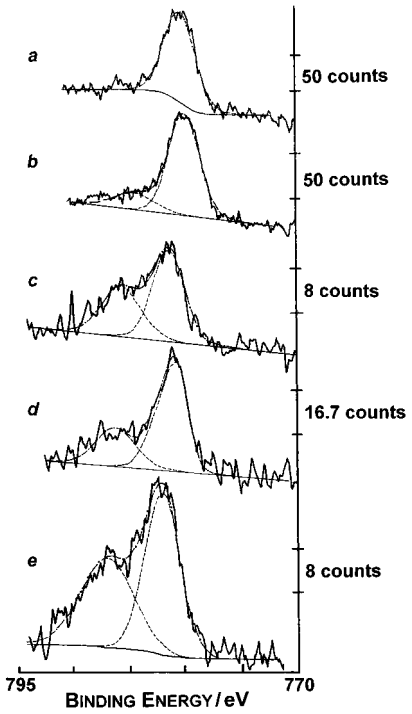

Figure 7. XPS studies of the Co $2p_{3/2}$ line for Co(salen) and {Co(salen)}NaY: (a) commercial Co(salen) rubbed into 2000 lines-per-inch gold grid; (b) commercial Co(salen) rubbed into 99.99% indium foil; (c) inertly prepared, CH_2Cl_2-exchanged {Co(salen)}NaY; (d) air-exposed, CH_2Cl_2-extracted {Co(salen)}NaY; (e) Co(II)-exchanged NaY, CoNaY.

{M(L)}Z be demonstrated, electrochemical methods should be useful for probing possible structural isomerization of zeolite-encapsulated complexes.

Although the UV−vis spectroscopic and voltammetric characterizations of {Co(salen)}NaY do not indicate any significant fraction of structural isomer, our XPS results do indicate differing chemical environments for near-surface Co present in our two basic preparations of {Co(salen)}NaY as compared to each other and to the pure complex. In Figure 7, the Co $2p_{3/2}$ XPS spectra are shown for Co(salen) and CH_2Cl_2-extracted {Co(salen)}NaY prepared either with air exposure or by inert handling à la Herron;[1] the latter material is electroinactive[20] and has the lowest near-surface Co/Al ratio of any of our {Co(salen)}-NaY specimens, Co/Al = 0.15.

Co(salen) has a Co $2p_{3/2}$ binding energy (BE) of 780.2 eV (see also Table 2). The susceptibility of this complex to interaction with oxygen-bearing moieties can be seen by comparing the spectra for this complex when rubbed into a Au grid to prepare the XPS specimen (Figure 7a) to that for the same powder rubbed into 99.99% indium foil, which contains a native surface oxide (Figure 7b). When placed on the oxide-bearing indium surface, the Co $2p_{3/2}$ line exhibits a high BE shoulder (shake-up or satellite structure) that is a feature common to the first-row transition metals when oxygen-bearing moieties are part of their chemical environment.[59] Although the BE of the main line does not shift, the satellite structure repeatably appears once Co(salen) contacts indium.

Synthesizing Co(salen) in NaY zeolite without rigorous attempts to do so under anhydrous and deoxygenated conditions leads to a solid that is indistinguishable by UV−vis from the inertly prepared material; yet the air-exposed material exhibits a higher near-surface concentration of Co and a small measure of electroactivity, as discussed above. Unlike UV−vis, the XPS structure and BE of the Co $2p_{3/2}$ lines for these materials are distinguishable, as can be seen by comparing the XPS spectra of the CH_2Cl_2-extracted versions of both solids (parts c and d of Figure 7). The BEs have shifted to higher values from that for the pure complex for both forms of {Co(salen)}NaY (see Table 2), but that for the inertly handled material is 1.3 eV higher than the value for pure complex (*vs* 0.6 eV for the air-exposed material) and shows a high BE satellite that is equal in intensity to the characteristic Co $2p_{3/2}$ line. The more oxygen-rich local environment around the zeolite-encapsulated Co(salen) center prepared under low H_2O and O_2 conditions is best explained by a close association of the Co with the oxygens of the zeolite lattice, an interaction that is unscreened by other sorbates.

The intensity of the high BE Co $2p_{3/2}$ satellite for {Co(salen)}-NaY prepared with air exposure is roughly 1/3 that of the total Co $2p_{3/2}$ intensity, showing the influence of the zeolite environment on the Co centers, even though the interaction is not as severe as that for the inertly prepared material. Furthermore, the chemical state of near-surface Co in {Co(salen)}NaY is not that seen for uncomplexed Co^{II} (Figure 7e) in CoNaY (which is the Co^{II}-exchanged starting form used to prepare {Co(salen)}-NaY). The Co $2p_{3/2}$ BE for CoNaY is 782.2 eV, which is 0.7 and 1.4 eV positive of that for air-exposed and inertly handled {Co(salen)}NaY, respectively. The oxygens of the zeolite framework have been shown to coordinate Co^{2+} in partially and fully dehydrated CoNaY,[60−62] so the enhancement of the satellite structure on the Co $2p_{3/2}$ line is expected as dehydration of the zeolite occurs in the ultrahigh vacuum chamber during the XPS experiment. As seen in Figure 7e, CoNaY also has, as observed for inertly handled {Co(salen)}NaY, an equivalent intensity for the satellite feature relative to the characteristic line.

Although there is more than one Co^{2+} per supercage in our Co(salen)-modified zeolite (and therefore some uncomplexed Co^{2+} ion), comparisons of the peak widths for {Co(salen)}-NaY *versus* Co(salen) (see Figure 7) and of the Co $2p_{3/2}$ BEs for {Co(salen)}NaY *versus* CoNaY (see Figure 7 and Table 2) indicate that the *near-surface* of {Co(salen)}NaY does not contain a significant (>10%) contribution from uncomplexed Co^{2+} ions. As discussed above, an equilibrium distribution of species from the external boundary into the zeolite crystal should not be expected after a "ship-in-a-bottle" synthesis. Calzaferri *et al*. observe that at high loadings of $\{[Ru(bpy)_3]^{2+}\}$NaY prepared via a "ship-in-a-bottle" synthesis, $[Ru(bpy)_3]^{2+}$ tends to accumulate to the external boundary.[57] This gradient of complex over ion in the near-surface region of {M(L)}Z is also indicate for our preparation of Co(salen)-modified NaY by the similarity of the XPS spectra for air-exposed {Co(salen)}NaY before and after aqueous Na^+-exchange (see Table 2).

Assignment of the Topological Isomer Undergoing Electron Transfer. The soundest evidence that the initial electroactive topological isomer in CH_2Cl_2-extracted, air-exposed {Co(salen)}NaY is actually $(\{Co(salen)\}NaY)_B$ can be seen by the loss of even minimal electroactivity after a second extraction with DMF when this material is characterized as either a ZME[20] or microheterogeneous dispersion. Notably, near-surface Co-(salen), *i.e*., $(\{Co(salen)\}NaY)_B$, although displaceable after 18−24 h of extraction or stirring with DMF,[20] appears to have hours-long tenacity at the zeolite boundary if no mechanical work is imparted to the zeolite crystals. This tenacity may indicate that Co(salen) residing in the outermost layer of complete supercages becomes unencapsulated with time (tens of hours) upon exposure to polar solvents. Co(salen) has a diameter of 8−9 Å, which means it is not rigorously size-excluded (or in this instance, size-included) by the 7.4 Å pore of the faujasite supercage. Barrer has determined that a kinetic diameter of

TABLE 2: X-ray Photoelectron Spectroscopic Binding Energies of Co $2p_{3/2}$ and Relative Areas of Satellite:Main Line for Co(salen), {Co(salen)}NaY, and $Co^{II}NaY$

sample	binding energy/eV	relative area of satellite:main line[a]
	Co(salen)[b]	
rubbed into 2000 lines/in. Au grid	780.2	0
rubbed into 99.99% indium foil	780.1	0.1
	{Co(salen)}NaY	
inertly prepared, CH_2Cl_2-extracted[c]	781.5	0.5
air-exposed, CH_2Cl_2-extracted[d,e]	780.7	0.3
air-exposed, CH_2Cl_2- and DMF-extracted[d,f]	780.7	0.3
air-exposed, CH_2Cl_2-extracted, DMF-stirred[d,g]	780.7	0.3
air-exposed, CH_2Cl_2-extracted, Na^+-exchanged[d,h]	780.7	0.3
	$Co^{II}NaY$	
	782.2	0.5

[a] Relative areas are corrected for instrumental factors; satellite and main peaks were deconvolved from the Co $2p_{3/2}$ envelope (see Figure 7). [b] As-received from Strem. [c] Synthesized and purified under N_2 atmosphere. [d] Synthesized in the presence of ambient air. [e] Soxhlet extracted with CH_2Cl_2 for 18 h. [f] Soxhlet extracted with CH_2Cl_2 for 18 h and Soxhlet extracted with DMF for 18 h. [g] Soxhlet extracted with CH_2Cl_2 for 18 h and stirred with DMF overnight. [h] Soxhlet extracted with CH_2Cl_2 for 18 h and ion exchanged with 0.1 M NaCl overnight.

>10 Å is required to block passage of a sorbate through the 12-ring window of X or Y.[63]

Conclusions

The cyclic voltammetry of {Co(salen)}NaY and {[Fe(bpy)$_3$]$^{2+}$}NaY was studied as a component of zeolite-modified electrodes or as a microheterogeneous dispersion. The amount of mechanical force imparted to the zeolite (as measured by the time of grinding or pressing of the {M(L)}Z) was found to markedly influence the observed electrochemical response. No voltammetric or UV−vis spectroscopic evidence was obtained for structural isomer formation during the synthesis of {Co(salen)}NaY by the flexible-ligand method, but the latter technique samples the bulk while the former sees only the near-exterior region of the redox-modified zeolite crystals. XPS does indicate that Co in boundary-sited {Co(salen)}NaY (expoxed to air/water during chelation with salen) interacts less strongly with the oxygens of the zeolite framework than the inertly handled material, and these complexes may be screened from the framework by a retained water molecule.

We urge that the terms proposed by Turro and Garcia-Garibay for assigning topological isomers of zeolite and probe solute[33] be adopted to clarify the discussion of electron transfer in redox-modified zeolites. The zeolite-encapsulated M(L)-species of Co(salen) and [Fe(bpy)$_3$]$^{2+}$ are electroactive as boundary-associated isomers that become truly external to the zeolite by protracted purification strategies or by imparting mechanical work to the zeolite to damage its surface. At the least, the mechanical work necessary to make most ZME formulations clearly affects the population (number and chemical state) of zeolite-associated redox probes giving rise to the electrochemical response. The use of ZMEs, where the redox-modified zeolite has undergone mechanical working during formulation of the ZME—especially when the electroactivity arises from only a minor fraction of the available species—may lead to artifactual electrochemistry uncharacteristic of the designed redox-modified zeolite.

Cyclic voltammetry of the transition metal complex-modified zeolite directly dispersed in nonaqueous electrolyte and addressed with a large surface area electrode captures a durable voltammetric response characteristic of the complex. Dispersion electrolysis of {M(L)}Z offers a method to observe the redox-modified zeolite in the absence of complications commonplace with ZMEs, since the carbon, binder, and electrode preparation necessary to form ZMEs are avoided. This characterization strategy also mimics the conditions used for preparative electrocatalysis using microheterogeneous dispersions of {M(L)}Z.[24,64]

All our electrochemical and analytical studies of these two examples of transition metal complex-modified zeolites support an extrazeolite redox mechanism involving an external surface topological isomer that is faradaically durable for hours in the absence of lattice damage.

Acknowledgment. We acknowledge Professor David N. Blauch (current address: Davidson College) for the preparation of {[Fe(bpy)$_3$]$^{2+}$}NaY, Dr. Michael W. Russell (Naval Research Laboratory, Code 6174) for assistance with the scanning electron microscopy experiments, Dr. Esther S. Takeuchi, Wilson Greatbatch, Ltd., for helpful discussions regarding the preparation of solid-state modified electrodes, and Professor Mark D. Baker, University of Guelph, for directing us to refs 48 and 49. C.A.B. gratefully acknowledges a National Research Council/Naval Research Laboratory postdoctoral fellowship award. This work was supported by the Office of Naval Research.

References and Notes

(1) Herron, N. *Inorg. Chem.* **1986**, *25*, 4714.

(2) (a) De Vos, D. E.; Thilbault-Starzyk, F.; Jacobs, P. A. *Angew. Chem., Int. Ed. Engl.* **1994**, *33*, 431. (b) Knops-Gerrits, P.-P.; De Vos, D. E.; Thibault-Starzyk, F.; Jacobs, P. A. *Nature* **1994**, *369*, 543. (c) Parton, R. F.; Vankelecom, I. F. J.; Casselman, M. J. A.; Bezoukhanova, C. P.; Uytterhoevan, J. B.; Jacobs, P. A. *Nature* **1994**, *370*, 541.

(3) Taylor, R. J.; Drago, R. S.; George, J. E. *J. Am. Chem. Soc.* **1989**, *111*, 6610.

(4) (a) Dutta, P. K.; Bowers, C.; *Langmuir* **1991**, *7*, 937. (b) Bowers, C.; Dutta, P. K. *J. Catal.* **1990**, *122*, 271. (c) Turbeville, W.; Robins, D. S.; Dutta, P. K. *J. Phys. Chem.* **1992**, *96*, 5024.

(5) (a) DeWilde, W.; Peeters, G.; Lunsford, J. H. *J. Phys. Chem.* **1980**, *84*, 2306. (b) Quayle, W. H.; Lunsford, J. H. *Inorg. Chem.* **1982**, *21*, 97. (c) Mizuno, K.; Lunsford, J. H. *Inorg. Chem.* **1983**, *22*, 3484. (d) Mizuno, K.; Imamura, S.; Lunsford, J. H. *Inorg. Chem.* **1984**, *23*, 510. (e) Imamura, S.; Lunsford, J. H. *Langmuir* **1985**, *1*, 326.

(6) De Vos, D. E.; Feijen, E. J. P.; Schoonheydt, R. A.; Jacobs, P. A. *J. Am. Chem. Soc.* **1994**, *116*, 4746.

(7) (a) Shaw, B. R.; Creasy, K. E. *J. Electroanal. Chem.* **1988**, *243*, 209. (b) Shaw, B. R.; Creasy, K. E.; Lanczycki, C. J.; Sargeant, J. A.; Tirhado, M. *J. Electrochem. Soc.* **1988**, *135*, 869.

(8) Gaillon, L.; Sajot, N.; Bedioui, F.; Devynck, J.; Balkus, K. J., Jr. *J. Electroanal. Chem.* **1993**, *45*, 157.

(9) Balkus, K. J., Jr.; Welch, A. A.; Gnade, B. E. *Zeolites* **1990**, *10*, 722.

(10) Bedioui, F.; De Boysson, E.; Devynck, J.; Balkus, K. J., Jr. *J. Chem. Soc., Faraday Trans.* **1991**, *87* (24), 3831.

(11) Bedioui, F.; De Boysson, E.; Devynck, J.; Balkus, K. J., Jr. *J. Electroanal. Chem.* **1991**, *315*, 313.

(12) Mesfar, K.; Carre, B.; Bedioui, F.; Devynck, J. *J. Mater. Chem.* **1993**, *3* (8), 873.

(13) Bedioui, F.; Roué, L.; Briot, E.; Devynck, J.; Bell, S. L.; Balkus, K. J., Jr. *J. Electroanal. Chem.* **1994**, *373*, 19.

(14) Bedioui, F.; Roué, L.; Devynck, J.; Balkus, K. J., Jr. *J. Electrochem. Soc.* **1994**, *141*, 3049.
(15) Bedioui, F.; Roué, L.; Devynck, J.; Balkus, K. J., Jr. *Stud. Surf. Sci. Catal.* **1994**, *84*, 917.
(16) With Koch Light high-purity 99.999+% powdered graphite: Balkus, K. J., Jr.; Gabrielov, A. G.; Bell, S. L.; Bedioui, F.; Roué, L.; Devynck, J. *Inorg. Chem.* **1994**, *33*, 67.
(17) Bedioui, F.; Roué, L.; Gaillon, L.; Devynck, J.; Bell, S. L.; Balkus, K. J., Jr. *Symposium on Chemically Modified Molecular Sieves*; Division of Petroleum Chemistry, American Chemical Society: Washington, DC, 1993; Vol. 38, p 529.
(18) Baker, M. D.; Senaratne, C.; Zhang, J. *J. Phys. Chem.* **1994**, *98*, 1668.
(19) Rolison, D. R. *Stud. Surf. Sci. Catal.* **1994**, *85*, 543, and references therein.
(20) Senaratne, C.; Baker, M. D.; Zhang, J.; Bessel, C. A.; Rolison, D. R. *J. Phys. Chem.* **1996**, *100*, 5849.
(21) Bedioui, F.; Devynck, J.; Balkus, K. J., Jr. *J. Phys. Chem.* **1996**, *100*, 8607.
(22) Rolison, D. R.; Bessel, C. A.; Baker, M. D.; Senaratne, C.; Zhang, J. *J. Phys. Chem.* **1996**, *100*, 8610.
(23) Folest, J.-C.; Duprilot, J.-M.; Perichon, J.; Robin, Y.; Devynck, J. *Tetrahedron Lett.* **1985**, *26*, 2633.
(24) Bessel, C. A.; Rolison, D. R. Manuscript in preparation.
(25) Balkus, K. J.; Jr.; Eissa, M.; Levado, R. *J. Am. Chem. Soc.* **1995**, *117*, 10753.
(26) Gould, S.; Strouse, G. F.; Meyer, T. J.; Sullivan, B. P. *Inorg. Chem.* **1991**, *30*, 2942.
(27) Li, J.; Calzaferri, G. *J. Chem. Soc., Chem. Commun.* **1993**, 1430.
(28) The estimate of *ca.* 1% electroactivity is a conservative estimate based on the known quantity of Co^{2+} exchanged into the zeolite. This estimate assumes that all the Co^{2+} sites ion exchanged into the zeolite form fully coordinated complexes with one salen ligand each.
(29) Kinoshita, K. *Carbon: Electrochemical and Physicochemical Properties*; Wiley: New York, 1988.
(30) Breck, D. W. *Zeolite Molecular Sieves*; Wiley: New York, 1974.
(31) *Intrazeolite Chemistry*; Stucky, G. D., Dwyer, F. G., Eds.; ACS Symposium Series 218; American Chemical Society: Washington, DC, 1983.
(32) Chen, N. Y.; Degnan, T. F., Jr.; Smith, C. M. *Molecular Transport and Reaction in Zeolites*; VCH: New York, 1994.
(33) Turro, N. J.; Garcia-Garibay, M. In *Photochemistry in Organized Media*; Ramamurthy, V., Ed.; VCH: New York, 1991; pp 1−38.
(34) Li, Z.; Mallouk, T. E. *J. Phys. Chem.* **1987**, *91*, 643.
(35) Li, Z.; Wang, C. M.; Persaud, L.; Mallouk, T. E. *Inorg. Chem.* **1988**, *92*, 2592.
(36) Li, Z.; Lai, C.; Mallouk, T. E. *Inorg. Chem.* **1989**, *28*, 178.
(37) Krueger, J. S.; Lai, C.; Li, Z.; Mayer, J. E.; Mallouk, T. E. In *Inclusion Phenomena and Molecular Recognition*; Atwood, J. E., Ed.; Plenum Press: New York, 1990; pp 365−378.
(38) Rolison, D. R. *Chem. Rev.* **1990**, *90*, 867.
(39) Baker, M. D.; Senaratne, C. In *Frontiers of Electrochemistry, Vol. 3: Electrochemistry of Novel Materials*; Lipkowski, J., Ross, P. N., Eds.; VCH: New York, 1994; pp 339−380.
(40) Gilman, J. J. *Science* **1996**, *274*, 65.
(41) Kvande, H.; Wahlbeck, P. G. *High Temp.−High Pressures* **1976**, *8*, 45.
(42) Fu, C. M.; Burns, R. P. *High Temp. Sci.* **1976**, *8*, 353.
(43) Pasternack, L.; Dagdigian, P. J. *J. Chem. Phys.* **1977**, *67*, 3854.
(44) (a) Kosanovic, C.; Bronic, J.; Cizmek, A.; Subotic, B.; Smit, I.; Stubicar, M.; Tonejc, A. *Zeolites* **1995**, *15*, 247. (b) Kosanovic, C.; Cizmek, A.; Subotic, B.; Smit, I.; Stubicar, M.; Tonejc, A. *Zeolites* **1995**, *15*, 51.
(45) Auroux, A.; Huang, M.; Kaliaguine, S. *Langmuir* **1996**, *12*, 4803.
(46) Szhulz-Ekloff, G.; Wright, D.; Grunze, M. *Zeolites* **1982**, *2*, 70.
(47) Bessel, C. A.; Rolison, D. R. *Stud. Surf. Sci. Catal.* **1995**, *98*, 114.
(48) Flanigen, E. M. In *Zeolite Chemistry and Catalysis*; Rabo, J. A., Ed.; American Chemical Society: Washington, DC, 1976; Vol. 171, pp 80−117.
(49) Freeman, D. C., Jr.; Stamires, D. N. *J. Chem. Phys.* **1961**, *35*, 799.
(50) It is also possible that the ligand-centered reductions use molecular orbitals spatially oriented such that limited *inter*cage electron exchange can occur between bipyridyls in adjacent supercages. The metal-centered process involves centers more physically separated and may represent only those complexes with a direct path to the electron conductor.
(51) Lever, A. B. P. In *Molecular Electrochemistry of Inorganic, Bioinorganic and Organometallic Compunds*; Pombeiro, A. J. L., McCleverty, J. A., Eds.; Kluwer: Amsterdam, 1993; pp 41−55, and references therein.
(52) (a) Eichhorn, E.; Speiser, B. *J. Electroanal. Chem.* **1994**, *365*, 207. (b) Eichhorn, E.; Ricker, A.; Speiser, B. *Angew. Chem.* **1992**, *104*, 1246.
(53) Kapturkiewicz, A.; Behr, B. *Inorg. Chim. Acta* **1983**, *69*, 247.
(54) In a recent comment by Ledney and Dutta[55] on the pioneering work with $\{[Ru(bpy)_3]^{2+}\}NaY$ by Lunsford and co-workers,[5] they interpret the electronic spectrum reported for $\{[Ru(bpy)_3]^{2+}\}NaY$[5] as indicative of the formation of ruthenium red, $[(NH_3)_5Ru-Ru(NH_3)_5-Ru(NH_3)_5]^{6+}$ arising from air exposure of the $Ru^{II}(NH_3)_6$-exchanged zeolite precursor.
(55) Ledney, M.; Dutta, P. K. *J. Am. Chem. Soc.* **1995**, *117*, 7687.
(56) The iron complex was believed to be present due to Fe^{II} impurities in the zeolite, since commercial zeolites may contain 0.2% Fe by weight.[5] By analogy, it is reasonable to conclude that $\{Fe(bpy)_3]^{2+}\}NaY$ species should form within the zeolite supercage during the preparation of $\{Ru(bpy)_3]^{2+}\}NaY$. Our ICP analyses show that it is difficult to remove the Fe impurity totally even after a pre-exchange of the commercial zeolite powder with 0.1 M NaCl.
(57) Lainé, P.; Lanz, M.; Calzaferri, G. *Inorg. Chem.* **1996**, *35*, 3514.
(58) We interpret the retention of oxygen affinity for {Co(salen)}NaY reported by Herron[1] to indicate that autoxidation of the zeolite-encapsulated Co(salen) did not occur. In hindsight, this lack of autooxidation offers further evidence for the inability of intrazeolite cage-to-cage electron transfer to occur. Herron's results indicate the advantages of site dilution as the individual complex molecules are separated due to the supercage structure of the zeolite.[1]
(59) Moulder, J. F.; Stickle, W. F.; Sobol, P. E.; Boben, K. D. *Handbook of X-ray Photoelectron Spectroscopy*; Chastain, J., Ed.; Perkin-Elmer Corp.: Eden Prairie, MN, 1992.
(60) Egerton, T. A.; Hagan, A.; Stone, F. S.; Vickerman, J. C. *J. Chem. Soc., Faraday Trans. 1* **1972**, *68*, 723.
(61) Hutta, P. J.; Lunsford, J. H. *J. Chem. Phys.* **1977**, *66*, 4716.
(62) Morrison, T. I.; Reis, A. H., Jr.; Gebert, E.; Iton, L. E.; Stucky, G. D.; Suib, S. L. *J. Chem. Phys.* **1980**, *72*, 6276.
(63) Barrer, R. M. *J. Inclusion Phenom.* **1983**, *1*, 105.
(64) deVismes, B.; Bedioui, F.; Devynck, J.; Bied-Charreton, C.; Perrée-Fauvet, M. *Nouv. J. Chim.* **1986**, *10*, 81.